

# Estimating 3D Crack Density Tensors and Effective Elastic and Conductive Properties from Crack Traces on 2D Cross-Sections

Yulia Pronina <sup>1, a)</sup>, Victoria Vialtseva <sup>1</sup>, and Mark Kachanov <sup>2, b)</sup>

<sup>1</sup>*St.Petersburg State University, 7/9 Universitetskaya nab., St. Petersburg, 199034 Russia.*

<sup>2</sup>*Tufts University, Medford, MA 02155, USA.*

<sup>a)</sup> Corresponding author: y.pronina@spbu.ru

<sup>b)</sup> mark.kachanov@tufts.edu

**Abstract.** The effective elastic and conductive properties of microcracked materials are controlled by parameters of the 3D crack density (scalar, in the isotropic case of random crack orientations, and tensor, in cases of non-random orientations). However, these parameters are difficult to be determined experimentally. On the other hand, the information on line crack traces on boundaries of specimens cut out of the material may be readily available. The present work develops the methodology of estimating the effective elastic and conductive properties of microcracked materials from the density and orientations of the mentioned traces. The accuracy of the obtained estimates is illustrated by numerical simulations.

## INTRODUCTION

The effective elastic and conductive properties of materials containing microcracks depend on crack concentration. The challenge encountered in this context is the identification of the proper crack density parameter in which terms the properties of interest are to be expressed. Several such parameters have been proposed in literature, including the *number* of cracks per unit area (see, e.g., [1]), the average spacing between cracks to the power  $-3$  [2], “crack porosity” that is routinely used in various applications. The question arises, which of the numerous parameters of crack concentration should be used?

The choice of this parameter depends on the physical property of interest (see the book of Kachanov and Sevostianov [3] for an in-detail discussion of this issue). Here, we consider the effective elastic and conductive properties of microcracked materials. Then, the classical parameter of crack density, first defined by Bristow [4] in the case of isotropy (random crack orientations), has the form

$$\rho_{3D} = \frac{1}{V} \sum_k r_k^3 . \quad (1)$$

In this formula, cracks are supposed to have the circular (penny) shape and  $r_k$  are the crack radii; the volume of averaging is denoted by  $V$ ; the notation “3D” indicates that the problem is three-dimensional. This formula takes the contributions of individual cracks proportionally to crack radii cubed, since that corresponds to their actual contributions to the effective properties (the compliance contribution of any flat crack is a product of the crack area and the average loading-induced displacement discontinuity across the crack that is proportional to the linear size of the crack). In its terms, the effective constants (normalized to the values for the isotropic virgin material, marked by subscripts 0) were derived by Bristow [4] in the non-interaction approximation (NIA) as follows:

$$\frac{E}{E_0} = \frac{1}{1 + (16/9) \left[ (1 - \nu_0^2) / (1 - 2\nu_0) \right] \rho_{3D}} , \quad (2)$$

$$\frac{G}{G_0} = \frac{1}{1 + (32/45) \left[ (1 - \nu_0) (5 - \nu_0) / (2 - \nu_0) \right] \rho_{3D}} , \quad (3)$$

$$\frac{k}{k_0} = \frac{1}{1 + (8/9)\rho_{3D}}. \quad (4)$$

where  $E$ ,  $G$  and  $\nu$  are Young's and shear moduli and Poisson's ratio; the conductivity is denoted by  $k$ . We mention that commonly used schemes, Mori-Tanaka's, differential, etc. are based on the NIA results. The NIA (formulated as above, without linearization in  $\rho_{3D}$ ) remains sufficiently accurate up to crack densities of at least  $0.12 - 0.15$ .

In anisotropic cases of non-random orientation distributions of cracks, the effective elastic properties are expressed in terms of the 2<sup>nd</sup> rank tensor  $\alpha = (1/V) \sum_k r_k^3 (\mathbf{n}\mathbf{n})^k$  and the 4<sup>th</sup> rank tensor  $\beta = (1/V) \sum_k r_k^3 (\mathbf{n}\mathbf{n}\mathbf{n}\mathbf{n})^k$  where  $\mathbf{n}^k$  is the unit normal to  $k$ -th crack. In their terms, the extra compliances due to cracks (additional to the ones of the isotropic matrix material) are given by Kachanov [5]:

$$\Delta S_{ijkl} = \frac{32(1-\nu_0^2)}{3(2-\nu_0) E_0} \left[ \frac{1}{4} (\delta_{ik}\alpha_{jl} + \delta_{il}\alpha_{jk} + \delta_{jk}\alpha_{il} + \delta_{jl}\alpha_{ik}) - \frac{\nu_0}{2} \beta_{ijkl} \right]. \quad (5)$$

Thus, in the case of isotropy, the elastic properties are expressed in terms of parameter (1) and, in cases of crack-induced anisotropy, in terms of tensors  $\alpha$  and  $\beta$ ; the virgin material is assumed to be isotropic in both cases. Note that similar, and somewhat simpler, formulas hold for the effective conductive properties, for which the  $\beta$ -tensor is irrelevant (see [3] for details). However, in experimental setting, estimation of these parameters is a challenging task. On the other hand, the information on crack traces, of lengths  $2l_k$ , on specimen faces may be readily available. In the present work, we discuss the extraction of information on 3D crack density from the crack traces.

In the case of isotropy, the relevant crack density parameter in the 2D setting is the sum

$$\rho_{2D} = \frac{1}{S} \sum_k l_k^2, \quad (6)$$

where  $S$  is the averaging area. In cases of crack-induced anisotropy, the orientation of crack traces should also be taken into account. The present work develops the step-by-step methodology of estimation of the effective elastic properties of a microcracked material from the observed crack traces on specimen boundaries (the properties of the matrix are assumed to be known).

Note that relations between 1D, 2D, and 3D microgeometry characteristics (volume fractions, area fractions in cross-sections, MIL, Minkowski's tensors, etc.) have been investigated in literature; see, for example, [6–8], and [9] for a more recent publication. However, they did not discuss the crack density parameters such as (1) and (6) or their tensor forms,  $\alpha$  and  $\beta$ . We emphasize that the proper crack density parameters for cracks do not involve their volume fractions (as seen from the definition of crack density in which terms the effective properties are expressed); see [10,11] for examples of application of these concepts. Therefore, the case of cracks should be considered separately (and not as a special case of inhomogeneities), and this constitutes the motivation for the present analysis.

## 2D–3D RELATIONS FOR CRACK DENSITIES

Here we provide the framework for estimating the 3D crack density,  $\rho_{3D}$ , from the 2D density of crack traces,  $\rho_{2D}$ , observed on cross-sections or specimen faces. We first consider the case of random crack orientations (overall isotropy) and then proceed to anisotropic case of several families of parallel cracks, at arbitrary angles with respect to each other; for in-detail analyses we refer to papers [12,13]. The presented  $\rho_{3D} - \rho_{2D}$  connections have to be understood in the statistical sense: firstly, the  $\rho_{3D} - \rho_{2D}$  connections discussed below are of statistical nature (they assume uniform distribution of cracks over their positions); secondly, the available input information on  $\rho_{2D}$  (for a finite set of cracks) may fluctuate from one specimen to another and the obtained estimates of  $\rho_{3D}$  would fluctuate about its actual value.

Note that the 2D–3D relations do not involve the crack radii and cover mixtures of cracks of diverse radii.

### Random Crack Orientations

We consider a volume element containing a representative set of penny-shaped cracks of random orientations (that produces isotropic effective elastic and conductive properties). We bisect the representative volume by a planar cross-

section and consider lines of intersection of cracks with this plane (any face of a cubic specimen cut out of the material Fig. 1).

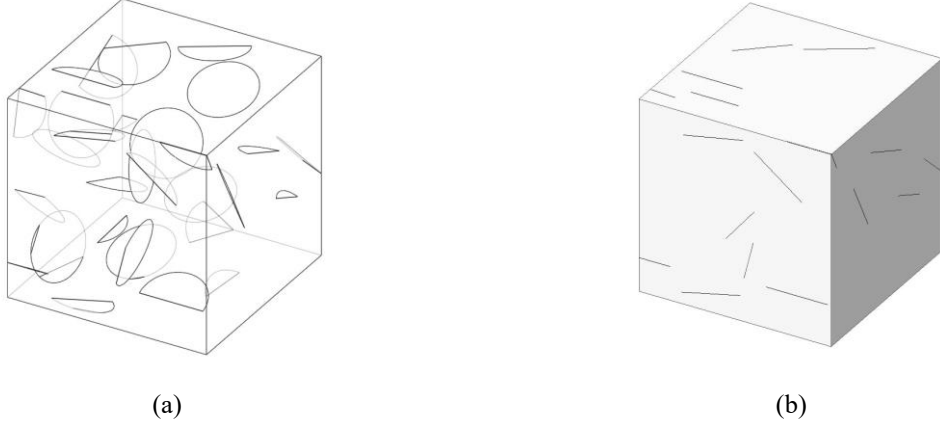


**FIGURE 1.** 3D arrays of cracks (a) and their traces on specimen boundaries (b); randomly oriented cracks.

Performing appropriate averaging over the crack orientations and over the distances of crack centers from the cross-section (assuming their uniform distributions), we arrive at the following formula

$$\rho_{3D} = \frac{3}{\pi} \rho_{2D}, \quad (7)$$

that explicitly relates the 3D crack density (that controls the effective properties) to the 2D density of crack traces observable on cross-section or specimen faces.

If the  $\rho_{2D}$  values are available for several cross-sections or specimen faces, averaging over the corresponding  $\rho_{3D}$  estimates will likely improve the accuracy.

### A Family of Parallel Cracks

We consider a volume element containing a representative set of parallel penny-shaped cracks (that produces anisotropic effective elastic and conductive properties). In this case, the density of crack traces on a given cross-section will depend on the orientation of this cross-section with respect to cracks. The 2<sup>nd</sup> rank tensor  $\alpha$  and the 4<sup>th</sup> rank tensor  $\beta$  entering into (2) may be represented as  $\alpha = \rho_{3D} \mathbf{n} \mathbf{n}$  and  $\beta = \rho_{3D} \mathbf{n} \mathbf{n} \mathbf{n} \mathbf{n}$  where  $\mathbf{n}$  is the unit normal to the crack system and  $\rho_{3D}$  is a scalar crack density (they are determined in the text to follow). This case constitutes the basic building block for analyses of more complex orientation distributions. We bisect the representative volume by three mutually perpendicular planes that may be treated as faces of a physical specimen (Fig. 2).

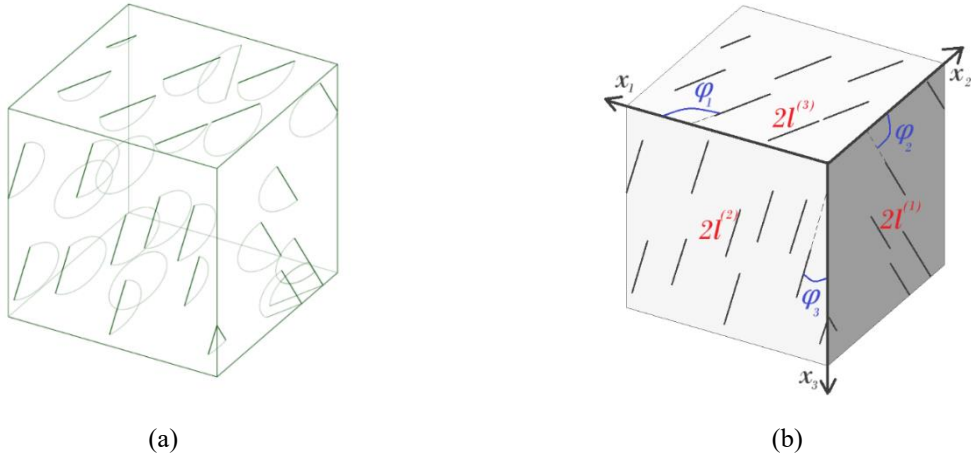


**FIGURE 2.** 3D arrays of cracks (a) and their traces on specimen boundaries (b); one family of parallel cracks. Superscripts  $(i)$  at  $l$  refer to faces with normals parallel to  $x_i$  axis.

The orientation of the crack family is found in a deterministic way; the unit normal to the cracks is given by any of the following three formulas [13]:

$$\begin{aligned} \mathbf{n} &= \frac{1}{\sqrt{1+\cot^2 \varphi_3 + \tan^2 \varphi_2}} \begin{pmatrix} -\cot \varphi_3 \\ -\tan \varphi_2 \\ 1 \end{pmatrix} = \frac{-\text{sign} \tan \varphi_3}{\sqrt{1+\cot^2 \varphi_1 + \tan^2 \varphi_3}} \begin{pmatrix} 1 \\ -\cot \varphi_1 \\ -\tan \varphi_3 \end{pmatrix}, \\ &= \frac{-\text{sign} \tan \varphi_2}{\sqrt{1+\cot^2 \varphi_2 + \tan^2 \varphi_1}} \begin{pmatrix} -\tan \varphi_1 \\ 1 \\ -\cot \varphi_2 \end{pmatrix} \end{aligned} \quad (8)$$

where  $\varphi_i$  are the angles between crack traces on the plane  $x_i x_{i+1}$  and the  $x_i$  axis (Fig.2).

The density  $\rho_{3D}$  may be estimated by any of the three formulas (obtained in terms of the mathematical expectations of the densities of cracks and their traces):

$$\rho_{3D} = \rho_{2D}^{(3)} \frac{3}{4} \sqrt{1 + \frac{\cos^2 \varphi_1}{\tan^2 \varphi_2}} = \rho_{2D}^{(1)} \frac{3}{4} \sqrt{1 + \frac{\cos^2 \varphi_2}{\tan^2 \varphi_3}} = \rho_{2D}^{(2)} \frac{3}{4} \sqrt{1 + \frac{\cos^2 \varphi_3}{\tan^2 \varphi_1}}, \quad (9)$$

where  $\rho_{2D}^{(i)}$  refers to the 2D density of crack traces on the corresponding cross-sections normal to the axis  $x_i$ . Averaging over all the estimates will improve the accuracy. Alternatively,  $\rho_{3D}$  can be determined from the following formula

$$\rho_{3D} = \frac{3}{4\sqrt{2}} \sqrt{\left(\rho_{2D}^{(1)}\right)^2 + \left(\rho_{2D}^{(2)}\right)^2 + \left(\rho_{2D}^{(3)}\right)^2}, \quad (10)$$

that may be preferable in cases when 2D densities of crack traces are available on three mutually perpendicular planes.

### Several Families of Parallel Cracks of Arbitrary Orientations

We consider the case of several families of parallel cracks inclined to each other at arbitrary angles (Fig. 3 shows the case of two families *A* and *B*).

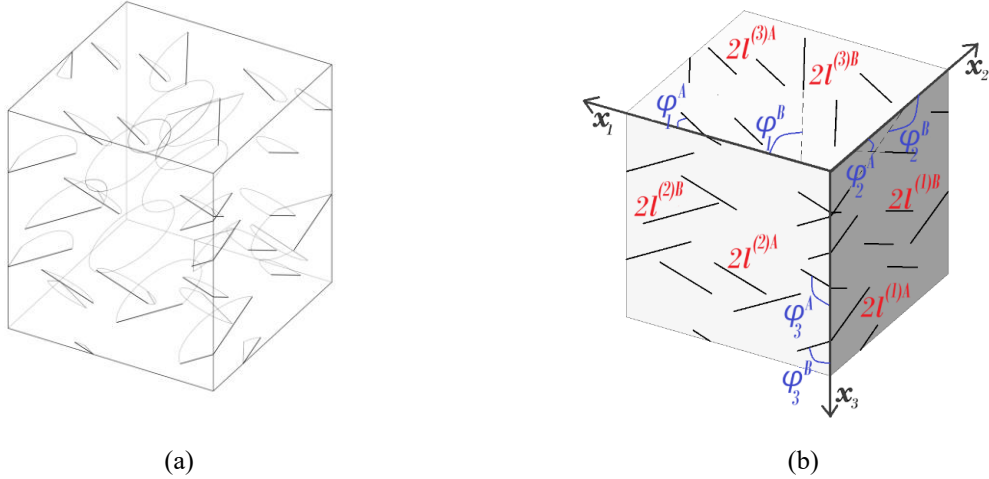


**FIGURE 3.** 3D arrays of cracks (a) and their traces on specimen boundaries (b); two families of parallel cracks. Superscripts (i)A or (i)B at  $l$  refer to faces with normals parallel to  $x_i$  axis, the traces belonging to crack family A or B.

The analysis of this case utilizes the results for a single crack family and involves the following tasks:

1. Identification, to which crack family each of the crack traces belongs, with simultaneous determination of the orientations of all the families,  $\mathbf{n}^M$ .
2. Determination of the partial scalar crack density  $\rho_{3D}^M$  for each  $M$ -th family.

3. Application of the superposition principle:  $\alpha = \sum_M \alpha^M$  and  $\beta = \sum_M \beta^M$

The criterion that angles  $\varphi_1$ ,  $\varphi_2$ , and  $\varphi_3$  corresponding to crack traces on three mutually perpendicular cross-sections belong to one family is given by the relation [13]:

$$\tan \varphi_1 \tan \varphi_2 \tan \varphi_3 = -1 \quad (11)$$

Verification of this criterion yields several combinations of three angles  $\varphi_i$ , each corresponding to a certain family. The orientation and a partial crack density for this family is determined by the formulas for one family of parallel cracks.

## The Procedure of Estimation of the Effective Properties

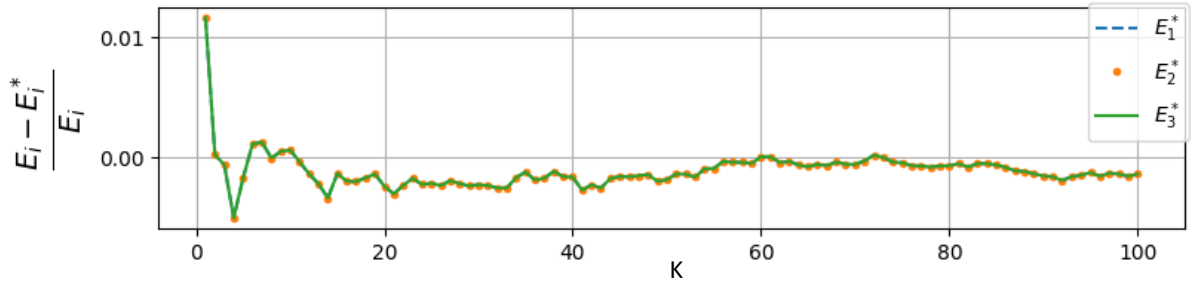
Thus, the following procedure of estimation of the effective properties can be suggested, in the general case of several systems of parallel cracks, as well as randomly oriented cracks:

1. In cases of several systems of parallel cracks: identification of each system and determination of their orientations ( $\mathbf{n}^M$ ), formulas (8) and (11).
2. Calculation of  $\rho_{2D}^M$  on available cross-sections for each crack system, formula (6).
3. For each available cross-section, estimation of partial densities  $\rho_{3D}^M$  for each crack family, formulas (9); formula (7) for randomly oriented cracks (isotropy).
4. Averaging the values of the crack density obtained from different cross-sections.
5. In cases of several crack systems: summation over all families.
6. Calculation of the effective elastic or conductive constants, using an appropriate scheme (NIA, for instance, formulas (2)–(5)).

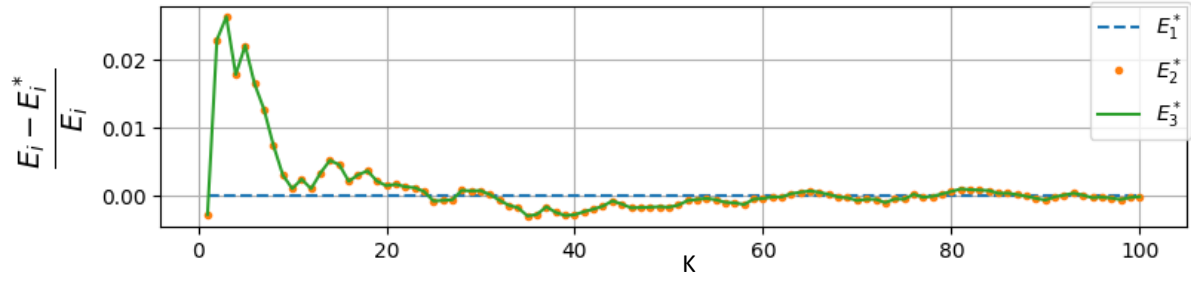
## NUMERICAL SIMULATIONS

Extensive numerical simulations for a number of finite crack sets have been performed in works [12,13] for the random transversely isotropic and non-random crack orientations, respectively. The simulations showed fluctuations of the estimates of  $\rho_{3D}$  about their actual (known a priori) values. In the present work, we combine estimates of  $\rho_{3D}$  with formulas for the effective elastic constants in the NIA. We present results on the fluctuations of the computed estimates of the effective Young's moduli, for one family of parallel cracks. Computations were performed for five different orientations of the crack family with respect to specimen faces. The discussed fluctuations, in their dependence on number  $K$  of specimens (over which the averaging, that followed averaging over six specimen faces, was performed) are shown in Fig. 4. Results show that the deviations are quite small, within 1%, even for small numbers of specimens (starting from about 20). Note that the deviations, being normalized to the values of the Young's moduli in the corresponding directions, are somewhat larger for the smallest moduli. The data of Table 1 demonstrate elastic anisotropy due to cracks in the isotropic matrix.

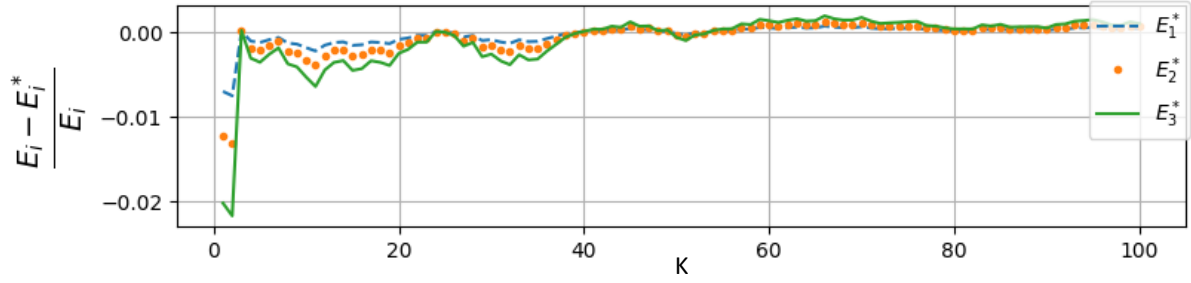
*Remark.* In the case 1 of Fig. 4 and Table 1, the cracks form equal angles with all coordinate axes. As a result, the three Young moduli in the coordinate directions are equal – in spite of the fact that the material is anisotropic – thus illustrating that the equality of Young's moduli in three orthogonal directions does not necessarily imply isotropy.



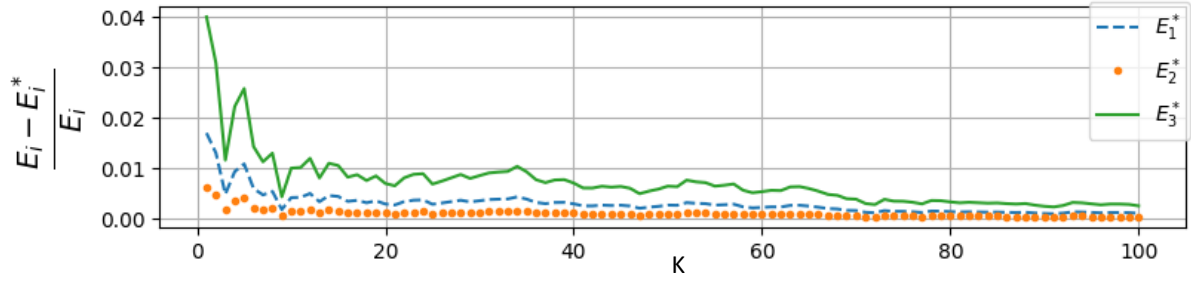
(a)



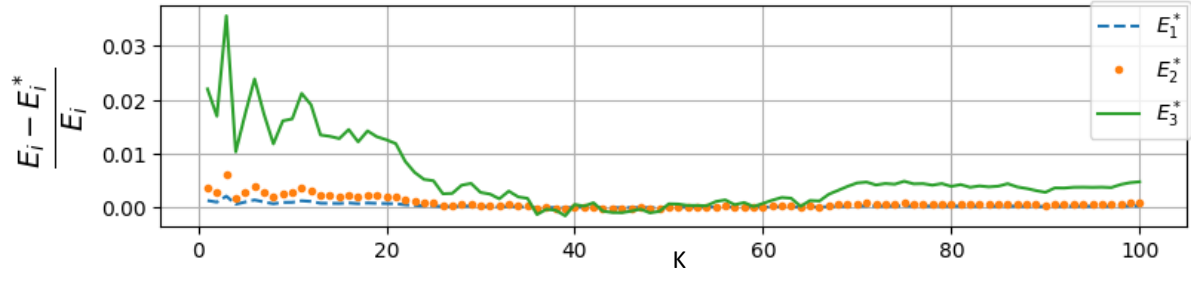
(b)



(c)



(d)



(e)

**FIGURE 4.** Dependence of the normalized fluctuations of estimates of Young's moduli on the number  $K$  of specimens over which the averaging was performed. The area of each face of a cubic specimen is  $1\text{cm}^2$ , crack radii are  $1\text{mm}$ , the number of cracks in a specimen  $N = 100$ . Properties of the virgin material:  $E_0 = 160\text{GPa}$ ,  $\nu_0 = 0.3$ .

**TABLE 1.** Young's moduli in  $x_i$  directions, for five orientations of one crack family with respect to  $x_i$ . Values of  $E_i^*$  and  $E_i$  are the computed estimates (from data on crack traces on six faces of each of 100 specimens) and the ones obtained using the actual value of  $\rho_{3D} = 0.1$ .

$\varphi_1, \varphi_2$	$E_1$	$E_2$	$E_3$	$E^*_1$	$E^*_2$	$E^*_3$
$3\pi/4, 3\pi/4$	135.50	135.50	135.50	135.70	135.70	136.70
$0, 3\pi/4$	160.00	126.57	126.57	160.00	126.60	126.60
$\pi/5, \pi/5$	147.33	137.99	124.05	147.28	137.90	123.93
$\pi/3, \pi/10$	142.49	153.56	117.72	142.34	153.50	117.42
$\pi/6, 9\pi/10$	157.24	152.08	111.52	157.19	151.93	110.86

## CONCLUDING REMARKS

The effective elastic and conductive properties are controlled by 3D crack density parameters, the scalar parameter (1) in the isotropic case of random crack orientations, and tensors  $\alpha$  and  $\beta$  in anisotropic cases of non-random orientations. However, experimental determination of these parameters is difficult. A methodology is developed of their estimates from the densities and orientations of crack traces on specimen boundaries. Computational simulations on finite sets of cracks combined with formulas for the effective properties showed that deviations of the estimates from the actual values are quite small, provided a sufficient total cross-sectional area is available.

This work establishes a methodology of determination of the effective elastic and conductive properties of microcracked materials, that can be used, in particular, as a monitoring tool.

## ACKNOWLEDGMENTS

The first two authors (YP and VV) acknowledge the support of the Russian Science Foundation, grant No 25-29-00565, <https://rscf.ru/project/25-29-00565/>

## REFERENCES

1. J. Bolivar, M. Frégonèse, J. Réthoré, C. Duret-Thual, and P. Combrade, Evaluation of multiple stress corrosion crack interactions by in-situ Digital Image Correlation. *Corros. Sci.* **128**, 120-129 (2017). <https://doi.org/10.1016/j.corsci.2017.09.001>
2. L. R. Botvina, A. I. Bolotnikov, and I. O. Sinev, Hierarchy of microcracks under cyclic and static loads. *Phys. Mesomech.* **23**(6), 466-476 (2020). <https://doi.org/10.1134/S1029959920060028>
3. M. Kachanov and I. Sevostianov, *Micromechanics of Materials, with Applications* (Springer, 2018, Series *Solid Mechanics and Its Applications*, edited by J. R. Barber), pp. 103–126, 245–249. <https://doi.org/10.1007/978-3-319-76204-3>
4. J. R. Bristow, Microcracks, and the static and dynamic elastic constants of annealed heavily cold-worked metals. *British J. Appl. Phys.* **11**, 81-85 (1960). <https://doi.org/10.1088/0508-3443/11/2/309>
5. M. Kachanov, Effective elastic properties of cracked solids: critical review of some basic concepts. *Appl. Mech. Rev.* **45**(8), 305–336 (1992).
6. M. Delesse, Procede mecanique pour determiner la composition des roches. *Annales des mines* **13**, 379-388 (1848) (in French).
7. R. L. Fullman, Measurement of particle sizes in opaque bodies. *J. Metals* **5**(3), 447-452 (1953). <https://doi.org/10.1007/BF03398971>
8. W. J. Whitehouse, The quantitative morphology of anisotropic trabecular bone. *J. Microsc.* **101**(2), 153-168 (1974). <https://doi.org/10.1111/j.1365-2818.1974.tb03878.x>
9. C. H. Arns, M. A. Knackstedt, and K. R. Mecke, Reconstructing complex materials via effective grain shapes. *Phys. Rev. Letters* **91**(21), 215506 (2003). <https://doi.org/10.1103/PhysRevLett.91.215506>
10. M. Kachanov, V. Mishakin, and Y. Pronina, On low cycle fatigue of austenitic steel. Part II: Extraction of information on microcrack density from a combination of the acoustic and eddy current data. *Int. J. Eng. Sci.* **169**, 103569 (2021). <https://doi.org/10.1016/j.ijengsci.2021.103569>

11. Y. Pronina, M. Narykova, and M. Kachanov, Relating stiffness changes in porous materials to the evolution of pore space. *Mech. Mater.* **202**, 105236 (2025). <https://doi.org/10.1016/j.mechmat.2024.105236>.
12. Y. Pronina and M. Kachanov, Estimating concentrations of cracks and platelets from their traces in 2D cross-sections. *Mech. Mater.* **180**, 104618 (2023). <https://doi.org/10.1016/j.mechmat.2023.104618>.
13. V. Vialtseva, Y. Pronina, and M. Kachanov, Finding densities and orientations of cracks and platelets from their traces in cross-sections, in anisotropic cases of non-random orientations. *Mech. Mater.* **209**, 105447 (2025). <https://doi.org/10.1016/j.mechmat.2025.105447>